Title : Geochemical implication of Eu isotope ratio in the anorthosite: a new evidence of Eu isotope fractionation by feldspar crystallization ”.

The authors: Seung-Gu Lee (Korea Institute of Geoscience and Mineral Resources, Daejeon 34132, Korea, sgl@kigam.re.kr)
Tsuyoshi Tanaka (Nagoya University, gotanaka@ob4.aitai.ne.jp)
Mijung Lee. (Korea Polar Research Institute, KIOST, mjlee@kopri.re.kr)

The corresponding author is as follows;
1) Name: Seung-Gu Lee
2) Address: Geology Division, Korea Institute of Geoscience and Mineral Resources, Daejeon 34132, Korea
3) TEL : +82-42-868-3376
4) e-mail: sgl@kigam.re.kr

Geochemical implication of Eu isotope ratio in the anorthosite: a new evidence of Eu isotope fractionation by feldspar crystallization

Seung-Gu Lee[1*] & Tsuyoshi Tanaka[2], Mi Jung Lee[3]

[1]Geology Division, Korea Institute of Geoscience and Mineral Resources, Daejeon 34132, Korea.
[2]Department of Earth and Environmental Sciences, Nagoya University, Nagoya 464-8601, Japan.
[3]Division of Polar Earth-System Sciences, Korea Polar Research Institute, Incheon 21990, Korea.

*e-mail: sgl@kigam.re.kr

Rare earth element geochemistry is important for understanding the evolution of the crust-mantle system. Europium (Eu) exists in divalent and trivalent states, and Eu^{2+} can be substituted for Ca^{2+} during plagioclase feldspar crystallization in reducing magmas. This leads to positive Eu anomaly in Ca-plagioclase-rich anorthosite derived from the mantle and negative Eu anomalies in fractionated silica-rich crustal rocks. But while Eu anomalies are well known, Eu has only two stable isotopes (^{151}Eu and ^{153}Eu), Eu isotope ratios have not been compared with Eu anomalies in igneous rocks. Here we report a systematic variation of the Eu isotope ratio ($\delta^{153/151}$Eu) from igneous rocks including anorthosite. This study finds a linear relationship between Eu anomalies and Eu isotope ratios in igneous rocks, with rhyolites and highly fractionated granites having large negative Eu anomalies and negative $\delta^{153/151}$Eu values but anorthosites having large positive Eu anomalies and positive $\delta^{153/151}$Eu values. Particularly, in the area of the highly fractionated igneous rocks with negative Eu anomaly, the Eu isotope fractionation proceeds with different slope according to the degree of magmatic differentiation in extrusive (volcanic) and intrusive (plutonic) rocks. Our finding reveals that Eu isotope fractionation in igneous rocks will provide new information related to magmatic differentiation and plagioclase feldspar fractional crystallization including anorthosite formation in the crust-mantle.

Key words: Eu isotope fractionation, Eu anomaly, magmatic differentiation, feldspar crystallization, anorthosite

Corresponding author: sgl@kigam.re.kr

INTRODUCTION

Rare earth elements (REEs) and their radiogenic isotope geochemistry (especially the ^{147}Sm-^{143}Nd and ^{138}La-^{138}Ce system) have provided abundant information for interpreting the geochemical evolution of Earth and extra-terrestrial materials as a result of their similar chemical behavior and continuously varying atomic masses of REEs. In particular, the geochemistry of chondrite-normalized REEs provides valuable petrogenetic information during the magma evolution processes such as partial melting from the mantle-derived rocks or crystallization from the magma (Coryell et al., 1963; Fowler and Doig, 1983; Masuda, 1962; Shearer and Papike, 1989; Weill and Drake, 1973). Most REEs have a stable (+3) state in natural systems; however, Eu can exist in both divalent and trivalent state under magmatic redox conditions, which indicates that the behavior of Eu during magmatic differentiation depends on the oxygen fugacity and crystallization of minerals (Burnham et al., 2015). Fractional crystallization is considered the dominant mechanism of magmatic differentiation and isolates crystallized-minerals from magma step by step (Bowen, 1928). Positive or negative Eu anomalies from the igneous rocks are produced by feldspar (particularly plagioclase) fractional crystallization with removal or accumulation, respectively, of plagioclase during magma evolution and have been interpreted as indicating the degree of differentiation of the source magma (Fowler and Doig, 1983; Shearer and Papike, 1989; Weill and Drake, 1973). For example, extremely large positive Eu anomaly in the anorthosite is due to concentration of Eu due to be substituted into the Ca site in plagioclase feldspar because the Ca^{2+} site in feldspar readily accepts Eu^{2+}. However, highly fractionated granite and high-silica rhyolite shows extremely large negative Eu anomalies.

Eu has only two isotopes, ^{151}Eu (47.81%) and ^{153}Eu (52.19%) (Rossman and Taylor, 1998). Though ^{151}Eu decayed to ^{147}Pm by α decay with the half-life $T_{1/2}=5\times10^{18}$yr (Belli et al., 2007), ^{151}Eu can be considered as a stable isotope in earth and solar system. In addition, recently, Lee and Tanaka (2021a) reported Eu isotope fractionation due to light Eu isotope enrichment (^{151}Eu) in highly fractionated granite and high-silica rhyolite with large negative Eu anomalies. The authors proposed that the heavier Eu isotope (^{153}Eu) might be enriched in anorthosite with large Eu positive anomaly due to Ca-feldspar crystallization.

At present, there have been no report on Eu anomaly and Eu isotope ratio in anorthosite including gabbro as well as the volcanic rocks such as andesite and trachyte. Therefore, here, we report the Eu isotope ratio and Eu anomaly among plutonic (intrusive) rocks such as anorthosites, gabbro and volcanic (extrusive) rocks such as andesite and trachyte, and compare the data of Eu isotope ratio from the igneous rocks such as basalt, rhyolite and granitoids.

The objective in this article is to find a possibility of a new tracer for studying the relationship between Eu anomaly in the chondrite-normalized REE pattern and the Eu isotope fractionation by comparing the magnitude of Eu anomaly and the degree of Eu isotope fractionation in various kinds of igneous rocks such as the extrusive rocks and intrusive rocks including anorthosite.

SAMPLES AND EXPERIMENTAL METHODS

Samples

In order to measure Eu isotope ratio of various kinds of igneous rocks, 49 igneous rock samples were used for Eu isotope ratio and REE abundance determination, of which 25 samples were geochemical reference materials purchased from the United States Geological Survey (USGS) and the Geological Survey of Japan (GSJ), while the others were anorthosites, granitoids and trachytes from Korea and Antarctica. The 25 geochemical reference materials in this study were as follows; Seven basalts (BCR2, BHVO2 and BIR1a purchased from the USGS; JB1a, JB1b, JB2 and JB3 from the GSJ), four andesites (AGV2 from USGS; JA1, JA2 and JA3 from GSJ), four rhyolites (RGM2 from USGS; JR1, JR2 and JR3 from GSJ), one diabase (W-2a from USGS), one dolerite (DNC1a from USGS), two gabbros (JGb1, JGb2 from GSJ), one syenite (STM2 from USGS), and five granites (G2 and GSP2 from USGS; JG1a, JG2 and JG3 from GSJ). The 24 rock samples from Korea and Antarctica are as follows; fourteen granites and five anorthosites from Korea, and five trachytes from Antarctica. Because there was no SRM trachyte, we collected five trachytes from Antarctica.

Sample digestion and determination of REE concentrations

The sample digestion procedure was based on the approach of Lee et al (2016). Approximately 100~200 mg of each sample powder was decomposed by a 2:1 mixture of 2~4 mL of concentrated HF (29M) and 1~2 mL of concentrated HNO_3 (16M) at ca. 160 ºC for more than 72 hours in 15 mL Savillex vial. After the addition of 0.1~0.2 mL of concentrated $HClO_4$, the decomposed sample solution was heated to dryness at ca. 180 ºC for more than 1 day. The cakes were re-dissolved by a mixture of 1 mL of concentrated HCl and 0.5 mL of concentrated HNO_3 at ca. 160 ºC for 1 day. Each sample solution was dried again, and diluted in 10 ml of 6 M HCl as a stock solution. Of this 10 ml stock solution, 0.5~1 ml stock solution was used to determine the rare earth element (REE) concentrations, and the remainder was used for determination of Eu isotope ratio.

Before Eu purification, we analyzed REE concentration of the sample using inductively coupled plasma mass spectrometry (ICP-MS, NexION350, Perkin Elmer) at KIGAM. Although Eu anomalies of the 25 geochemical reference rocks (USGS, GSJ) have previously been characterized, we also reanalyzed their REE abundances for comparison. The analyzed REE data from the geochemical reference sample powders (SRM) agreed with the recommended values within 5~10%.

Experimental procedures for determination of Eu isotope ratio

Recently, Lee and Tanaka (2019, 2021b) developed a method for determining highly precise and accurate Eu isotope ratio using Sm spike as an internal standard in combination with standard-sample-standard bracketing mass bias correction (C-SSBIN). In addition, Lee and Tanaka (2021a, 2021b) also showed that incomplete Eu purification from the geological material lead to change in the Eu isotope ratio, that is, pseudo-fractionation of Eu isotope ratio.

In this study, Eu was separated from the obtained REE fraction using 0.12 M 2-hydroxyisobutyric acid (HIBA) with the pH adjusted to ~4.60 (Lee and Tanaka, 2019, 2021b). To minimize isobaric interference because we used Sm which was prepared from ultrapure Sm_2O_3 produced by Alfa Aesar as a spike for normalization of Eu isotopes, we always checked for tailing of both Gd and Sm.

Eu isotope ratios were measured using multicollector inductively coupled plasma mass spectrometry (MC-ICP-MS; Neptune Plus, Thermo Fisher Scientific Ltd.) in static mode with nine Faraday cups at KIGAM. The instrument was tuned to achieve high sensitivity while maintaining flattened square peaks and stable signals enough to ensure accurate measurements. The gain on each Faraday cup was monitored daily to ensure normalization of its efficiency. Sample dilution for Eu isotope measurement by MC-ICP-MS was performed with 2% HNO_3 which was prepared from 60% ultrapure HNO_3 (Merck, Darmstadt, Germany) and DIW (Milli-Q system, Millipore, Milford, USA). We used a diluted solution of NIST 3117a (10,000 μg/mL, Lot No. 120705) as an in-house standard solution for comparison of the Eu isotope ratios.

The isotopes ^{147}Sm(L4), ^{149}Sm(L3), ^{150}Sm(L2), ^{151}Eu(L1), ^{152}Sm(C), ^{153}Eu(H1), ^{154}Sm(H2), ^{155}Gd(H3), and ^{157}Gd(H4) were monitored simultaneously using nine Faraday cups for Sm normalization and Gd interference correction by the Gd matrix (Lee and Tanaka, 2021b). Data acquisition consisted of 1 block of 50 cycles with an integration time of 4.194 seconds and a sample aspiration rate of 80-100 μL/min. Peak centering was performed at the beginning of each analysis and 250 s of washout time was used between sample measurements. Blanks were checked during, before, and after each sample measurement. Operating conditions and data acquisition parameters, including cup configuration, are the same as Lee and Tanaka (2021a, 2021b). In determination of Eu isotope ratio, we used ^{147}Sm/^{149}Sm (1.0868, Dubois et al., 1992) for normalization to obtain an optimum value of Eu isotope fractionation from the natural materials because of isobar matrix problem by ^{154}Gd due to incomplete separation from the geological rock during ^{150}Sm/^{154}Sm normalization (Lee and Tanaka, 2021a, 2021b). Eu isotope fractionation is represented in standard δ-notation in per mil relative to the NIST3117a Eu standard solution as follows: $\delta^{153/151}\mathrm{Eu} = 1{,}000 \times [(^{153}\mathrm{Eu}/^{151}\mathrm{Eu}_{\mathrm{sample}})/(^{153}\mathrm{Eu}/^{151}\mathrm{Eu}_{\mathrm{NIST3117a}}) - 1]$.

RESULTS

Rare Earth Element concentration in the extrusive rocks and intrusive rocks

In order to validate the accuracy of the REE data in this study, we determined REE concentrations of 25 geochemical standard reference materials (SRM) produced by USGS and GSJ. REE abundances of the geochemical reference materials from the United States of Geological Survey (USGS) and Geological Survey of Japan (GSJ) measured in this study are reported in Supplementary Table S1. In addition, REE concentrations of the local igneous rocks in Korea and Antarctica including anorthosite are presented in Table 1.

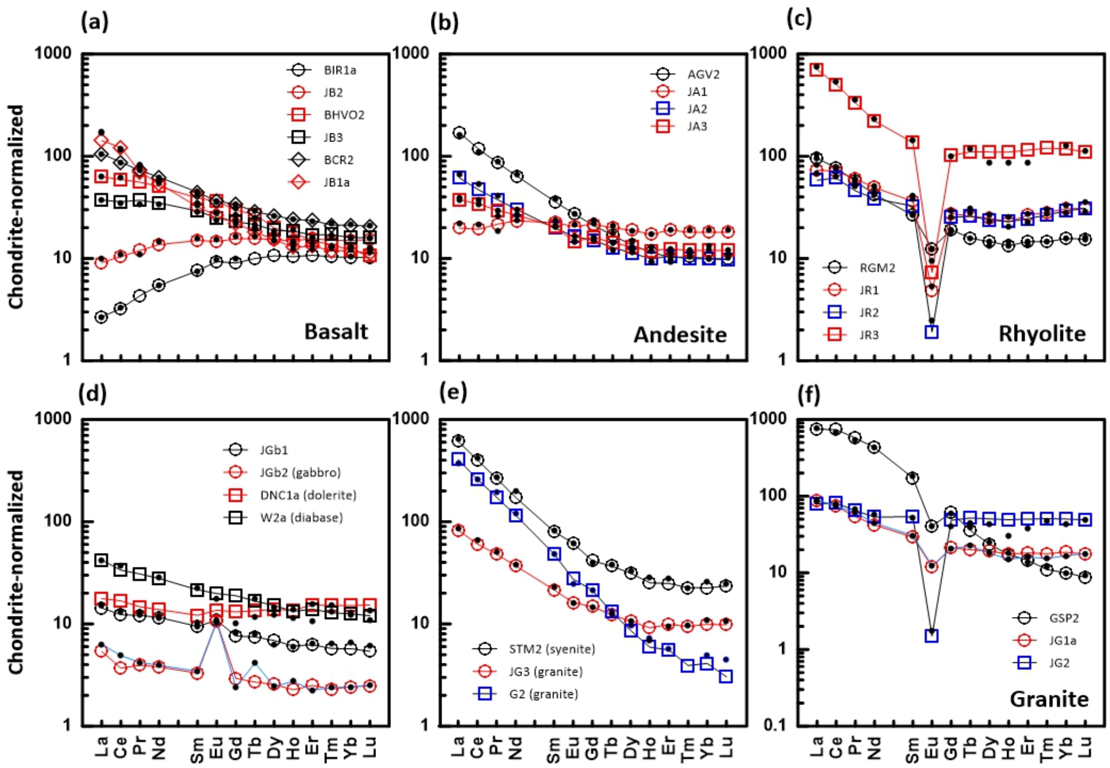

Fig. 1. Chondrite (McDonough and Sun, 1995)-normalized REE pattern of standard reference materials (SRMs) of USGS and GSJ. (a), (b) and (c) are SRMs for volcanic (extrusive) rocks whereas (d), (e) and (f) are SRMs for intrusive rocks such as gabbro, diabase and granitoids. In this paper, we classified dolerite and diabase as plutonic rocks rather than volcanic rocks. The REE abundances of all SRMs were re-measured from this study (see Table S1). REE patterns by solid black dots were drawn by recommended values for each SRM from USGS and GSJ.

Figures 1 and 2 are chondrite-normalized REE patterns for SRMs and Korea and Antarctic igneous rocks, respectively. In Fig. 1, REE patterns from the volcanic rocks such as basalt, andesite and rhyolite were drawn in Fig. 1a~1c whereas those from the plutonic rocks such as gabbro and granitoids were drawn in Fig. 1d~1f. The chondrite-normalized REE patterns from various kinds of igneous rocks in Figs. 1 and 2 clearly show variation of the magnitude of Eu anomaly due to feldspar crystallization during magmatic differentiation even though they are not cogenetic igneous rocks. Particularly, the anorthosites in Fig. 2a has strikingly large Eu positive anomaly.

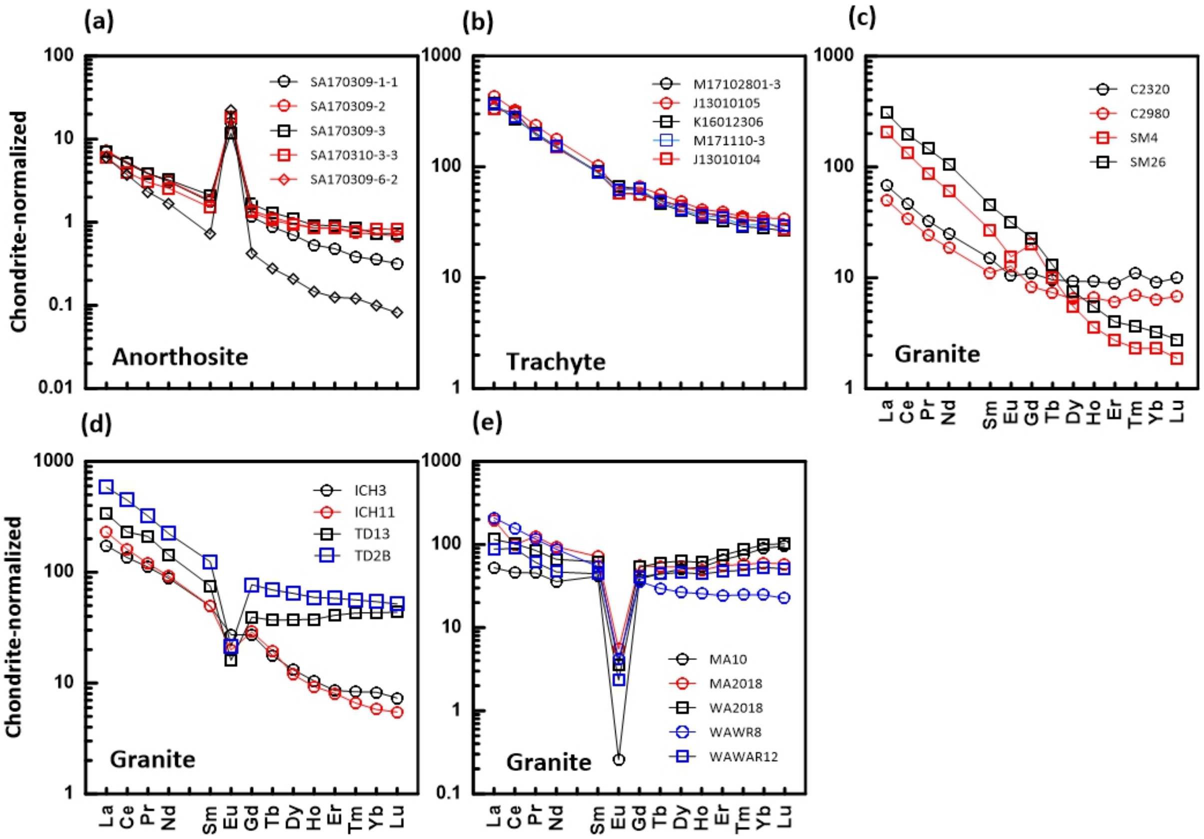

Fig. 2. Chondrite (McDonough and Sun, 1995)-normalized REE pattern of Korean and Antarctic igneous rocks. Except (b) trachyte, the others are all collected from Korea. Trachyte was collected from Antarctica. The REE abundances of Korean anorthosites and Anrarctic trachytes were re-measured from this study. REE patterns of Koean granites are from Lee et al. (2004, 2006, 2008, 2013).

Eu isotope ratio in in the extrusive rocks and intrusive rocks

Eu isotope ratio and magnitude of Eu anomaly from various kinds of the igneous rocks in this study are presented in Table 2. For comparison, in Table 2, we divided the samples into SRM and local igneous rocks. The $^{153/151}$Eu value of anorthosite all are positive, indicating that heavier Eu isotope (^{153}Eu) was enriched compared to lighter Eu isotope (^{151}Eu).

DISCUSSION

A major objective of this study is to examine the relationship between the magnitude of Eu anomaly due to feldspar crystallization during magmatic differentiation and Eu isotope differentiation. Therefore, we first compared the magnitudes of Eu anomalies with the $\delta^{153/151}$Eu values of the 49 samples to investigate the possibility that Eu isotope fractionation had occurred during magma differentiation (Fig. 3). Figure 3 illustrates three geochemical characteristics of Eu isotope fractionation as follows; 1) The $\delta^{153/151}$Eu values of the highly fractionated granites and rhyolites with extremely large negative Eu anomaly are negative, whereas the anorthosites with extremely large positive Eu anomaly show relatively large positive $\delta^{153/151}$Eu values. This contrast indicates that the highly fractionated igneous rocks, which are emplaced from felsic magma in an upper crustal environment, were enriched in the lighter Eu isotope (^{151}Eu), whereas Ca-plagioclase-rich anorthosite, which are derived from the mafic magma in a lower crustal environment, were enriched in the heavier Eu isotope (^{153}Eu). 2) The $\delta^{153/151}$Eu value in the igneous rock varies systematically with magnitude of the Eu anomaly. 3) Another interesting feature of the Eu fractionation trends in the volcanic and plutonic rocks is that intrusive rocks (red symbols in Fig. 3) and extrusive rocks (green and blue symbols in Fig. 3) are distributed with different slopes.

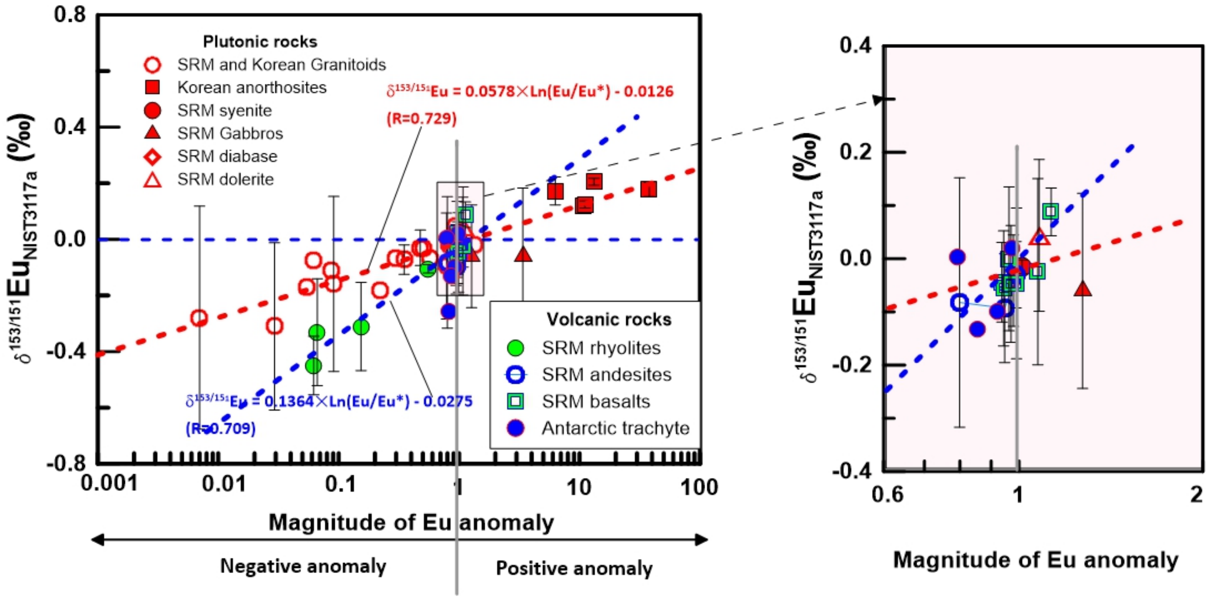

Fig. 3. Variation of Eu isotope ratio according to magnitudes of Eu anomalies from igneous rocks. The error bars represent uncertainties (2SD) of the average $\delta^{153/151}$Eu values from some of igneous rock samples.

Ismail et al. (1998) employed cation exchange chromatography and concluded that an isotope effect in the Eu^{2+}/ Eu^{3+} exchange reaction may occur in aqueous solutions; specifically, they found isotope effects in which the heavier isotope ^{153}Eu is enriched in Eu^{2+} in the Eu^{2+}/Eu^{3+} electron exchange system. The positive Eu anomaly in anorthosite can easily be explained by the substitution of Eu^{2+} for Ca^{2+} in plagioclase during differentiation of the anorthositic (primary) magma either in the upper mantle or at the lower crust. Therefore, we can suggest that the enrichment of heavier isotope ^{153}Eu in the anorthosites with large positive Eu anomaly should be explained due to isotope effects in Eu^{2+}/Eu^{3+} electron exchange system during Ca-plagioclase accumulation in the anorthositic magma. Moreover, the systematic correlation between Eu isotope fractionation and the magnitudes of Eu anomaly from the fractionated igneous rocks and anorthosites indicates that Eu isotope fractionation was closely related to magmatic differentiation processes such as feldspar fractional crystallization.

Another interesting finding in Figure 3 is that the trend of Eu isotope fractionation between the extrusive volcanic rocks and intrusive plutonic rocks seems to be different. Although more in-depth studies are needed in the future, the existence of such different slope can be interpreted as indicating the possibility that the Eu isotope fractionation in intrusive and extrusive rocks occurred by different mechanism or geochemical environment. The behavior of Eu is known to be determined by temperature and oxygen fugacity (Weill and Drake, 1973), and Philpotts and Schnetler (1968) and Philpotts (1970) suggested that Eu anomalies are controlled by crystal chemistry and magmatic oxidation potential. Dauphas et al. (2014) showed that equilibrium iron isotope fractionation is controlled mainly by the redox and structural conditions in magma and suggested that magmatic differentiation is the main driver of Fe isotope fractionation in felsic magmas. In addition, Dauphas et al. (2014) proposed that stable isotopes from heterovalent elements, including Eu, may show isotopic variations in bulk rocks controlled by the redox and structural conditions in the magma. Therefore, we also may be able to consider a possibility that a slight difference of the $\delta^{153/151}$Eu values in the plutonic rocks and volcanic rocks may be due to the oxidation potential in the magma. Further study is needed to clarify the relationship between Eu isotope fractionation and oxidation potential in an intrusive magmatic system.

Besides Eu isotope fractionation, recently, several research groups reported isotope fractionation study of REEs like Ce, Nd, Sm, Dy, Er and Yb (Moynier et al., 2006; Nakada et al., 2013; Shollenberger and Brebbecka, 2020; Hu et al., 2021). This means that combined information using chondrite-normalized REE pattern, radiogenic isotope geochemistry and δREE will provide new constraints for understanding more clearly the processes in our Earth and Planetary system such as redox conditions in the mantle and/or crust, early earth formation, and crust/mantle differentiation.

CONCLUSION

We compared the magnitude of Eu anomaly in the chondrite-normalized REE pattern from various kinds of igneous rocks such as the extrusive rocks and intrusive rocks including anorthosite.and their Eu isotope ratio from the fractionation. The anorthosites having large positive Eu anomalies show a geochemical characteristic of a heavier Eu isotope (^{153}Eu) enrichment (i.e., positive $\delta^{153/151}$Eu value) whereas the rhyolites and highly fractionated granites having large negative Eu anomalies show a geochemical characteristic of a lighter Eu isotope (^{151}Eu) enrichment (i.e., negative $\delta^{153/151}$Eu value). Particularly, our results clearly showed that variation of the magnitude of Eu anomaly and Eu isotope fractionation in igneous rocks has systematic correlation, suggesting that Eu isotope fractionation in igneous rocks should be produced by feldspar crystallization during magma evolution. In addition, the Eu isotope fractionation in the highly fractionated volcanic and plutonic rocks was proceeded with different trend, implying that the Eu isotope fractionation from the intrusive and extrusive magma in the crustal environment may occur under different mechanism or geochemical environment.

Acknowledgements This work was supported by the grants from the Principal Research Fund of the Korea Institute of Geoscience and Mineral Resources (GP2020-003, GP2021-006) and the National Research Foundation of Korea (NRF) grant funded by the Korea government (MSIT) (2020R1F1A1075924, NP2020-012) to S-G. Lee. This work was also partly supported by grants from Korea Polar Research Institute Project (PE21050) to M.J. Lee.

REFERENCES

Belli, P., Bernabei, R., Cappella, F., Cerulli, R., Dai, C. J., Danevich, F.A., d'Angelo, A., Incicchitti, A., Kobychev, V. V., Nagorny, S. S., Nisi, S., Nozzoli, F., Prosperi, D., Tretyak, V. I., Turchenko, S. S. (2007) Search for α decay of natural Europium, *Nucl. Phy. A* **789**, 15–19. (https://doi.org/10.1016/j.nuclphysa.2007.03.001)

Burnham, A. D., Berry, A. J., Halse, F. R., Schofield, P. F., Cibin, G. and Mosselmans, J. F. W. (2015) The oxidation state of europium in silicate melts as a function of oxygen fugacity, composition and temperature. *Chem. Geol.* **411**, 248–259. (https://doi.org/10.1016/j.chemgeo.2015.07.002)

Bowen, N. L. (1928) The Evolution of the Igneous Rocks, Princeton University.

Coryell, C. G., Chase, J. W. and Winchester, J. W. (1963) A procedure for geochemical interpretation of terrestrial rare-earth abundance patterns. *J. Geophys. Res*. **68**, 559–566. (https://doi.org/10.1029/JZ068i002p00559)

Dauphas, N., Roskosz, M., Alp, E. E., Neuville, D. R., Hu, M. Y., Sio, C. K. Tissot, F. L. H., Zhao, J. L. Tissandier, L., Médard, E. and Cordier, C. (2014) Magma redox and structural controls on iron isotope variations in Earth's mantle and crust. *Earth Planet. Sci. Lett*. **398**, 127–140. (https://doi.org/10.1016/j.epsl.2014.04.033)

Dubois, J. C., Retail, G. and Cesario, J. (1992) Isotopic analysis of rare earth elements by total vaporization of samples in thermal ionization mass spectrometry, *Int. J. Mass Spectrom. Ion Proc*. **120**, 163–317. (https://doi.org/10.1016/0168-1176(92)85046-3)

Fowler, A. D. and Doig, R. (1983) The significance of europium anomalies in the REE spectra of granites and pegmatites, Mont Laurier, Quebec. *Geochim. Cosmochim. Acta* **47**, 1131–1137. (https://doi.org/10.1016/0016-7037(83)90243-0)

Hu, J. Y., Dauphas, N., Tissot, F. L. H., Yokochi, R., Ireland, T. J., Zhang, Z. and Davis, A. M., (2021) Heating events in the nascent solar system recorded by rare earth element isotopic fractionation in refractory inclusions. *Sci. Adv*. **7**, eabc2962. (DOI: 10.1126/sciadv.abc2962)

Ismail, I. M., Nomura, M. and Fujii, Y. (1998) Isotope effects of europium in ligand exchange system and electron exchange system using ion-exchange displacement chromatography, *J. Chromatogr. A.* **808**, 185–191. (https://doi.org/10.1016/S0021-9673(98)00116-2)

Lee, S-G., Asahara, Y., Tanaka, T., Lee, S. R. and Lee, T. (2013) Geochemical significance of the Rb-Sr, La-Ce and Sm-Nd isotope systems in A-type rocks with REE tetrad patterns and negative Eu and Ce anomalies: The Cretaceous Muamsa and Weolaksan granites, South Korea. *Chem. der Erde* **73**, 75–88. (https://doi.org/10.1016/j.chemer.2012.11.008)

Lee, S-G., Kim, J-K., Yang, D-Y. and Kim, J-Y. (2004) Provenance of the river sediments in Icheon area based on the grain size and their geochemical characteristics. *J. Geol. Soc. Korea* **40**, 409–429 (in Korean with English abstract).

Lee, S-G., Kim, T., Tanaka, T, Lee, S-R. and Lee, J-I. (2016) Effect on the Measurement of Trace Element by Pressure Bomb and Conventional Teflon Vial Methods in the Digestion Technique. *J. Petrol. Soc. Korea* **25**, 1–13 (with English abstract in Korean).

Lee, S-G.. Kim, T-K , Lee, J-S. and Song, Y-H. (2006) Rb-Sr Isotope Geochemistry in Seokmodo Granitoids and Hot Spring, Gwangwha: An Application of Sr Isotope for Clarifying the Source of Hot Spring. *J. Petrol. Soc. Korea* **15**, 60–71 (with English abstract in Korean).

Lee, S-G., Lee, T.J. and Shin, H. (2008) Rb-Sr age and its geochemical implication of granitoid cores from deep borehole at Pohang area, Korea, *J. Geol. Soc. Korea* **44**, 409–423 (with English abstract in Korean).

Lee, S-G. and Tanaka, T. (2019) Determination of Eu isotopic ratio by multi-collector inductively coupled plasma mass spectrometry using a Sm internal standard. *Spectrochim. Acta Part B* **156**, 42–50. (https://doi.org/10.1016/j.sab.2019.04.011)

Lee, S-G. and Tanaka, T. (2021a) Eu isotope fractionation in highly fractionated igneous rocks with large Eu negative anomaly. *Geochem. J.* **55/6**, e9–e17. (https://doi.org/10.2343/geochemj.2.0631)

Lee, S-G. and Tanaka, T. (2021b) Gd matrix effects on Eu isotope fractionation using MC-ICP-MS: Optimizing Europium isotope ratio measurements in geological rock samples. *Int. J. Mass Spec*. **156**, 42–50. (https://doi.org/10.1016/j.ijms.2021.116668)

Lee, Y., Cho, M., Cheong, W.S. and Yi, K. (2014) A massif-type (~1.86 Ga) anorthosite complex in the Yeongnam Massif, Korea: late-orogenic emplacement associated with the mantle delamination in the North China Craton. *Terra Nova.* **26**, 408–416.

Masuda, A. (1962) Regularities in variation of relative abundances of lanthanide elements and attempt to analyze separation-index patterns of some minerals. *J. Earth Sci. Nagoya Univ*. **10**, 173–187.

McDonough, W. F. and Sun, S-S. (1995) The composition of the Earth, *Chem. Geol.***120**, 15–19. (https://doi.org/10.1016/0009-2541(94)00140-4)

Millet, M-A., Dauphas, N., Greber, N. D., Burton, K. W., Dale, C. W., Debret, B., Macpherson, C. G., Nowell, G. M. and Williams, H. M. (2016) Titanium stable isotope investigation of magmatic processes on the Earth and Moon. *Earth Planet. Sci. Lett*. **449**, 197–205. (https://doi.org/10.1016/j.epsl.2016.05.039)

Moynier, F., Bouvier, A., Blichert-Toft, J., Telouk, P., Gasperini, D. and Albarède, F. (2006) Europium isotopic variations in Allende CAIs and the nature of mass-dependent fractionation in the solar nebula. *Geochim Cosmochim Acta* **70**, 4287–4294. (https://doi.org/10.1016/j.gca.2006.06.1371)

Nakada, R., Tanamizu, M. and Takahashi, Y. (2013) Difference in the stable isotopic fractionations of Ce, Nd, and Sm during adsorption on iron and manganese oxides and its interpretation based on their local structures. *Geochim. Cosmochim. Acta* **121**, 105–119. (https://doi.org/10.1016/j.gca.2013.07.014)

Philpotts, J. A. (1970) Redox estimation from a calculation of Eu^{2+} and Eu^{3+} concentrations in natural phases. *Earth Planet. Sci. Lett*. **9**, 257–268. (https://doi.org/10.1016/0012-821X(70)90036-1)

Philpotts, J. A. and Schnetzler, C. C. (1968) Europium anomalies and the genesis of basalt. *Chem. Geol.* **3**, 5–13. (https://doi.org/10.1016/0009-2541(68)90009-0)

Shearer, C. K. and Papike, J. J. (1989) Is plagioclase removal responsible for the negative Eu anomaly in the source regions of mare basalts? *Geochim. Cosmochim. Acta* **53**, 3331–3336. (https://doi.org/10.1016/0016-7037(89)90113-0)

Schaen, A. J., Schoene, B., Dufek, J., Singer, B. S., Eddy, M. P. Jicha, B. R. and Cottle, J. M. (2021) Transient rhyolite melt extraction to produce a shallow granitic pluton. *Sci. Adv*. **7**: eabf0604. (DOI: 10.1126/sciadv.abf0604)

Shollenberger, Q. R. and Brennecka, G. A. (2020) Dy, Er, and Yb isotope compositions of meteorites and their components: Constraints on presolar carriers of the rare earth elements. *Earth Planet. Sci. Lett*. **529**, 115866. (https://doi.org/10.1016/j.epsl.2019.115866)

Weill, D. F., Drake, M. J. (1973) Europium Anomaly in Plagioclase Feldspar: Experimental Results and Semiquantitative Model. *Science* **180**, 1059–1060. (DOI: 10.1126/science.180.4090.1059)

Figure Cations

Fig. 1. Chondrite (McDonough and Sun, 1995)-normalized REE pattern of standard reference materials (SRMs) of USGS and GSJ. (a), (b) and (c) are SRMs for volcanic (extrusive) rocks whereas (d), (e) and (f) are SRMs for intrusive rocks such as gabbro, diabase and granitoids. In this paper, we classified dolerite and diabase as plutonic rocks rather than volcanic rocks. The REE abundances of all SRMs were re-measured from this study (see Table S1). REE patterns by solid black dots were drawn by recommended values for each SRM from USGS and GSJ.

Fig. 2. Chondrite (McDonough and Sun, 1995)-normalized REE pattern of Korean and Antarctic igneous rocks. Except (b) trachyte, the others are all collected from Korea. Trachyte was collected from Antarctica. The REE abundances of Korean anorthosites and Antarctic trachytes were re-measured from this study. REE patterns of Korean granites are from Lee et al. (2004, 2006, 2008, 2013).

Fig. 3. Variation of Eu isotope ratio according to magnitudes of Eu anomalies from igneous rocks. The error bars represent uncertainties (2SD) of the average $\delta^{153/151}$Eu values from some of igneous rock samples.

Table 1 . Rare earth element concentrations of igneous rocks

Rock Type	Area	Sample Name	La (ppm)	Ce (ppm)	Pr (ppm)	Nd (ppm)	Sm (ppm)	Eu (ppm)	Gd (ppm)	Tb (ppm)	Dy (ppm)
Trachyte	Mt. Melbourne (Antarctica)	M17102801-3	78.42	190.5	18.12	68.07	13.17	3.26	11.29	1.80	10.81
		J13010105	103.3	198.7	21.92	80.38	15.09	3.46	13.09	2.04	11.92
		K16012306	87.78	164.8	18.74	70.02	13.35	3.76	12.51	1.68	9.89
		M171110-03	86.93	172.4	18.10	70.93	12.98	3.49	12.50	1.77	10.11
		J13010104	78.42	190.5	18.12	68.07	13.17	3.26	11.29	1.80	10.81
Anorthosite	Sancheong (Korea)	SA20170309 1-1	1.64	3.25	0.36	1.41	0.26	0.87	0.23	0.03	0.17
		SA20170309 -2	1.73	3.18	0.36	1.43	0.27	0.99	0.28	0.04	0.24
		SA20170309-3	1.65	3.12	0.35	1.47	0.31	0.66	0.33	0.05	0.27
		SA20170309-6-2	1.42	2.27	0.22	0.77	0.11	1.24	0.08	0.01	0.05
		SA20170310 3-3	1.41	2.45	0.28	1.17	0.22	1.04	0.26	0.04	0.23
Granitoid	Muamsa-Weolaksan (Korea)	MA10	12.42	28.12	4.23	16.35	6.12	0.01	7.61	1.62	12.39
		WAWR12	20.97	54.60	5.67	21.40	6.56	0.13	8.13	1.59	11.35
		WAWR8	49.60	96.30	10.80	40.20	8.07	0.24	7.15	1.07	6.56
		MA2018	46.39	60.86	11.64	42.91	10.59	0.31	11.08	1.93	13.23
		WA2018	27.30	62.63	7.88	30.31	9.17	0.20	10.63	2.17	15.58
	Seokmodo (Korea)	SM4	48.70	81.50	8.11	27.70	4.00	0.87	4.00	0.36	1.35
		SM26	72.80	120.80	13.50	48.50	6.66	1.78	4.55	0.47	1.85
	Icheon (Korea)	ICH3	41.20	83.00	10.32	40.28	7.29	1.54	5.42	0.64	3.24
		ICH11	54.50	98.70	11.10	42.10	7.34	1.12	5.75	0.71	2.92
	Pohang (Korea)	C2320	16.15	28.50	3.03	11.35	2.20	0.59	2.18	0.35	2.30
		C2980	11.95	20.93	2.24	8.49	1.64	0.72	1.65	0.27	1.58
	Taedo (Korea)	TD13	79.97	141.0	19.52	65.33	11.11	0.90	7.83	1.33	9.16
		TD2B	138.3	273.9	29.76	101.8	18.36	1.21	15.36	2.50	15.84

Ho (ppm)	Er (ppm)	Tm (ppm)	Yb (ppm)	Lu (ppm)	Reference
2.10	5.79	0.83	5.14	0.66	This study
2.26	6.25	0.88	5.57	0.83	
1.88	5.19	0.71	4.50	0.65	
1.99	5.58	0.73	4.88	0.72	
2.10	5.79	0.83	5.14	0.66	
0.03	0.08	0.01	0.06	0.01	
0.05	0.13	0.02	0.12	0.02	
0.05	0.15	0.02	0.12	0.02	
0.01	0.02	0.00	0.02	0.002	
0.05	0.14	0.02	0.13	0.02	
2.92	10.46	1.86	14.55	2.34	
2.41	7.57	1.21	8.54	1.25	
1.40	3.88	0.61	3.97	0.56	
2.66	8.95	1.42	9.67	1.43	
3.31	11.85	2.14	16.01	2.51	
0.20	0.44	0.06	0.37	0.05	Lee et al. (2006)
0.30	0.64	0.09	0.52	0.07	
0.57	1.37	0.21	1.33	0.18	Lee et al. (2004)
0.51	1.29	0.16	0.93	0.13	
0.50	1.42	0.28	1.46	0.25	Lee et al. (2008)
0.36	0.97	0.17	1.03	0.17	
2.05	6.54	1.06	6.96	1.07	This study
3.23	9.31	1.39	8.73	1.27	

Table 2. Eu isotope ratio from SRM and local igneous rocks in this study

Extrusive (volcanic) rocks

Rock type	Basalt (SRM)							Andesite (SRM)				Trachyte (Antarctica)					Rhyolite (SRM)				SRM		Gabbro (SRM)	
Sample name	**BCR2**[1]	**JB2**	**JB1a**	**JB1b**	**JB3**	**BHVO2**	**BIR1a**	**JA1**	**JA2**	**JA3**	**AGV2**	**M1710 2801-3**	**J1301 0105**	**K1601 2306**	**M1711 10-03**	**J1301 0104**	**JR2**	**JR1**	**RGM2**	**JR3**	**W2a**	**DNC1a**	**JGb2**	**JGb1**
Eu/Eu*[2]	0.94	0.96	0.99	0.94	0.97	1.07	1.13	0.93	0.95	0.80	0.99	0.24	0.16	0.94	1.01	0.25	0.07	0.15	0.56	0.06	0.98	1.08	3.38	1.27
$\delta^{153/151}$Eu[3]	-0.08	-0.02	-0.05	-0.06	-0.05	-0.02	0.09	-0.13	-0.09	-0.08	-0.03	-0.27	-0.41	-0.07	-0.05	-0.54	-0.37	-0.28	-0.10	-0.50	-0.03	0.04	0.08	-0.07
2SD	0.04 (n=12)	0.14 (n=10)	0.14 (n=8)	0.11 (n=2)	0.10 (n=14)	0.17 (n=4)	0.05 (n=7)	0.20 (n=7)	0.09 (n=7)	0.23 (n=7)	0.12 (n=3)	-	-	-	-	-	-	0.08 (n=2)	0.02 (n=3)	0.27 (n=4)	0.04 (n=4)	0.14 (n=6)	0.23 (n=11)	0.19 (n=7)

Intrusive (plutonic) rocks

Rock type	Anorthosite					Granitoids													Granitoids (SRM)					
Sample name	SA1703 09-1-1	SA1703 09-2	SA1703 09-3	SA1703 09-6-2	SA1703 10-3-3	MA10	***MA 2018***[4]	***WAWR 2018***	***WAWR 12***	WAWR 8	***SM4***	***SM26***	***ICH11***	***ICH3***	***C2320***	***C2980***	TD13	TD2B	**STM2**	**JG1a**	**G2**	**JG3**	**GSP2**	**JG2**
Eu/Eu*	37.71	12.28	6.29	12.98	9.77	0.01	***0.09***	***0.06***	***0.06***	0.09	***0.66***	***0.93***	***0.51***	***0.72***	***0.81***	***1.32***	0.30	0.21	1.01	0.48	0.79	0.89	0.35	0.03
$\delta^{153/151}$Eu	0.118	0.125	0.172	0.184	0.244	-0.28	***-0.11***	***-0.07***	***-0.17***	-0.16	***0.05***	***0.00***	***-0.03***	***-0.07***	***-0.02***	***-0.02***	-0.07	-0.18	0.00	-0.03	-0.10	-0.01	-0.07	-0.31
2SD	-	0.01 (n=2)	0.05 (n=3)	0.03 (n=3)	-	0.40 (n=2)	-	-	-	0.31 (n=4)	-	-	-	-	-	-	-	-	0.06 (n=5)	0.06 (n=13)	0.19 (n=4)	0.04 (n=10)	0.05 (n=17)	0.30 (n=6)

1) The samples of Bold character are SRMs of USGS and GSJ.

2) The magnitude of Eu anomaly is defined as s the ratio Eu_N/Eu^* where Eu* is SQRT(Sm_N x Gd_N).

3) Eu isotope ratio normalized by ^{147}Sm-^{149}Sm isotope pair (Lee and Tanaka, 2021a, 2021b).

4) Eu isotope data (Bold Italic numbers) are from Lee and Tanaka (2021a)

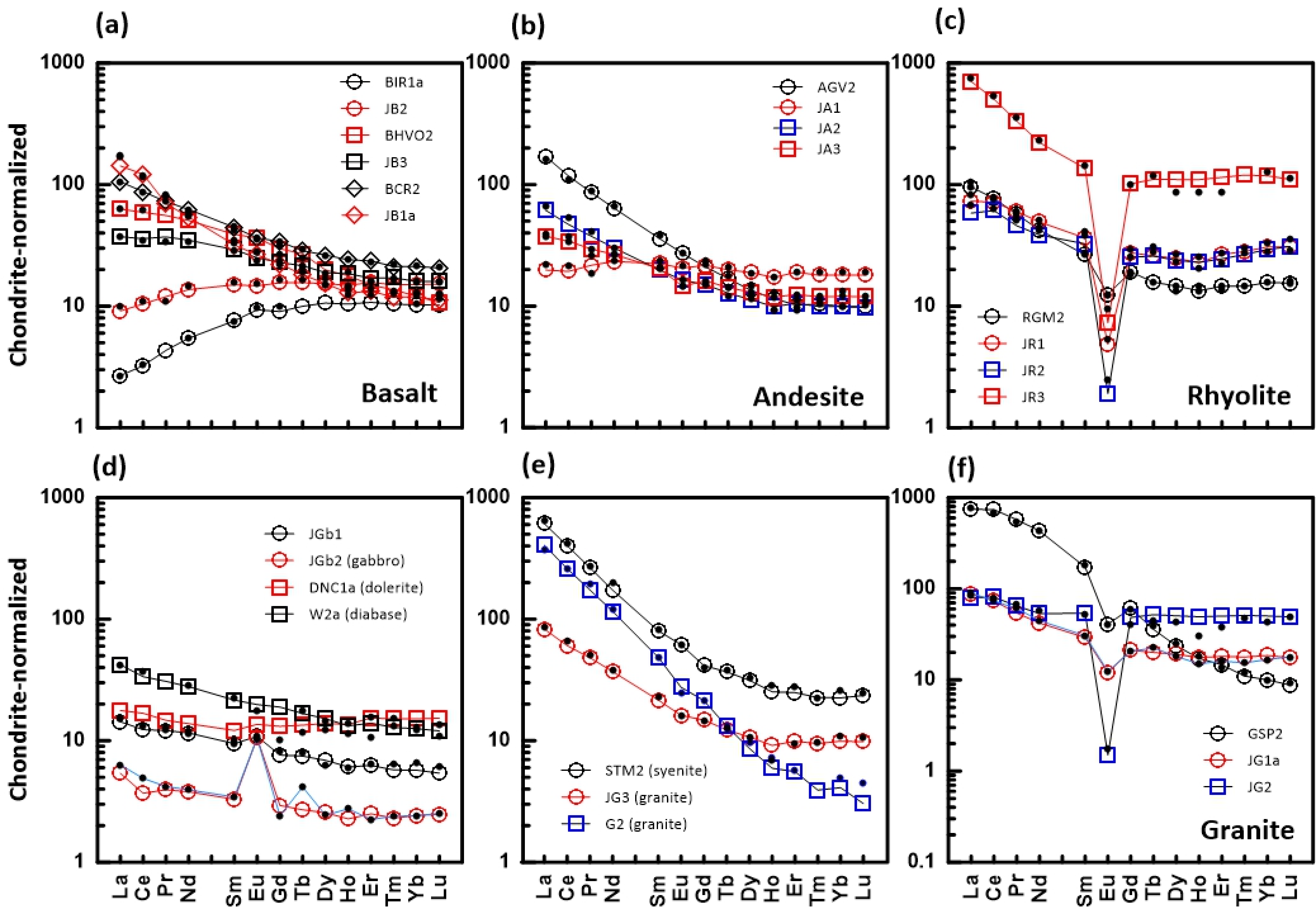

(a)
(b)
(c)
(d)
(e)
(f)
Chondrite-normalized
BIR1a
JB2
BHVO2
JB3
BCR2
JB1a
Basalt
AGV2
JA1
JA2
JA3
Andesite
RGM2
JR1
JR2
JR3
Rhyolite
JGb1
JGb2 (gabbro)
DNC1a (dolerite)
W2a (diabase)
STM2 (syenite)
JG3 (granite)
G2 (granite)
GSP2
JG1a
JG2
Granite
La Ce Pr Nd Sm Eu Gd Tb Dy Ho Er Tm Yb Lu

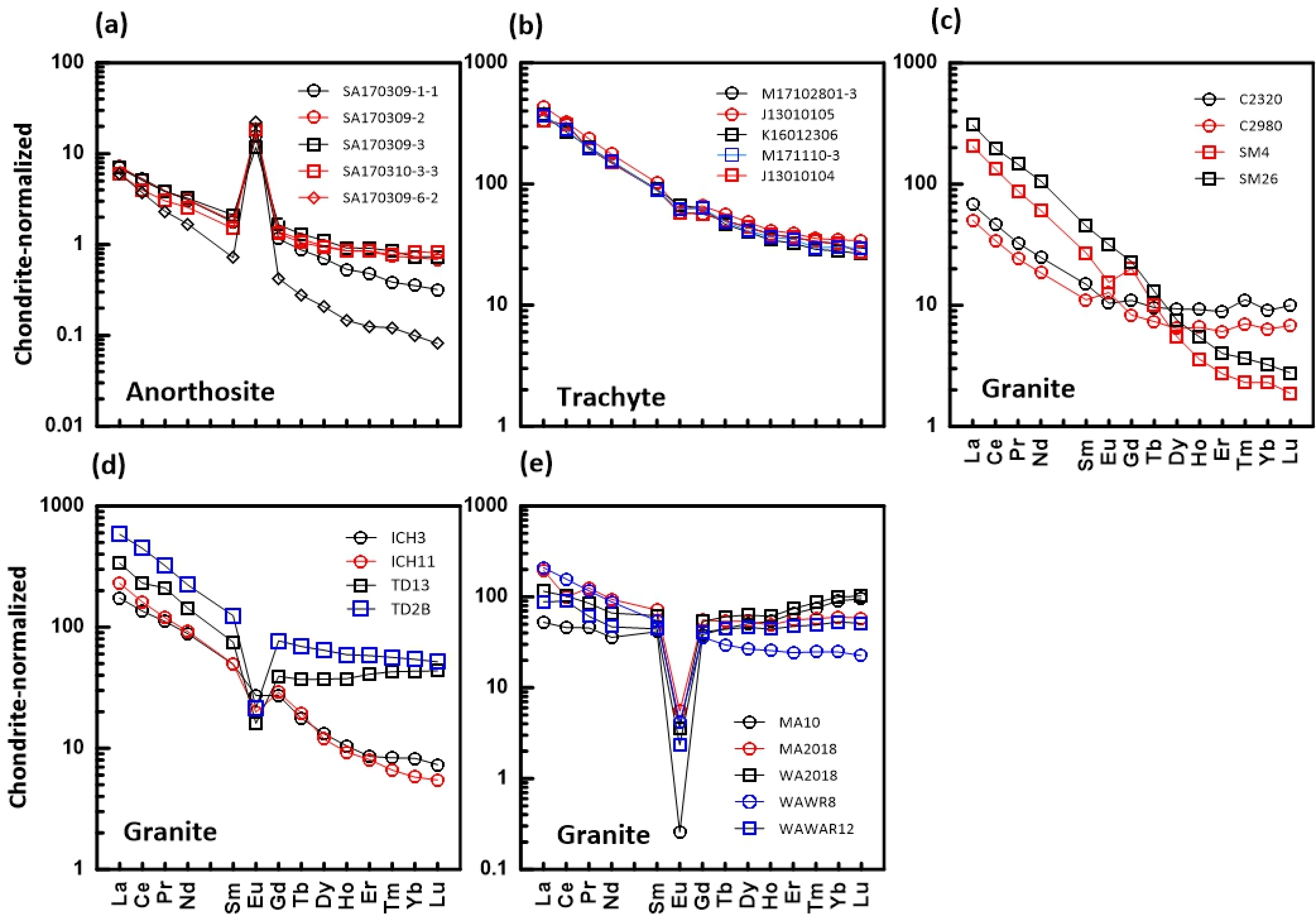

(a)
(b)
(c)
(d)
(e)
Chondrite-normalized
SA170309-1-1
SA170309-2
SA170309-3
SA170310-3-3
SA170309-6-2
Anorthosite
M17102801-3
J13010105
K16012306
M171110-3
J13010104
Trachyte
C2320
C2980
SM4
SM26
Granite
ICH3
ICH11
TD13
TD2B
MA10
MA2018
WA2018
WAWR8
WAWAR12
La Ce Pr Nd Sm Eu Gd Tb Dy Ho Er Tm Yb Lu

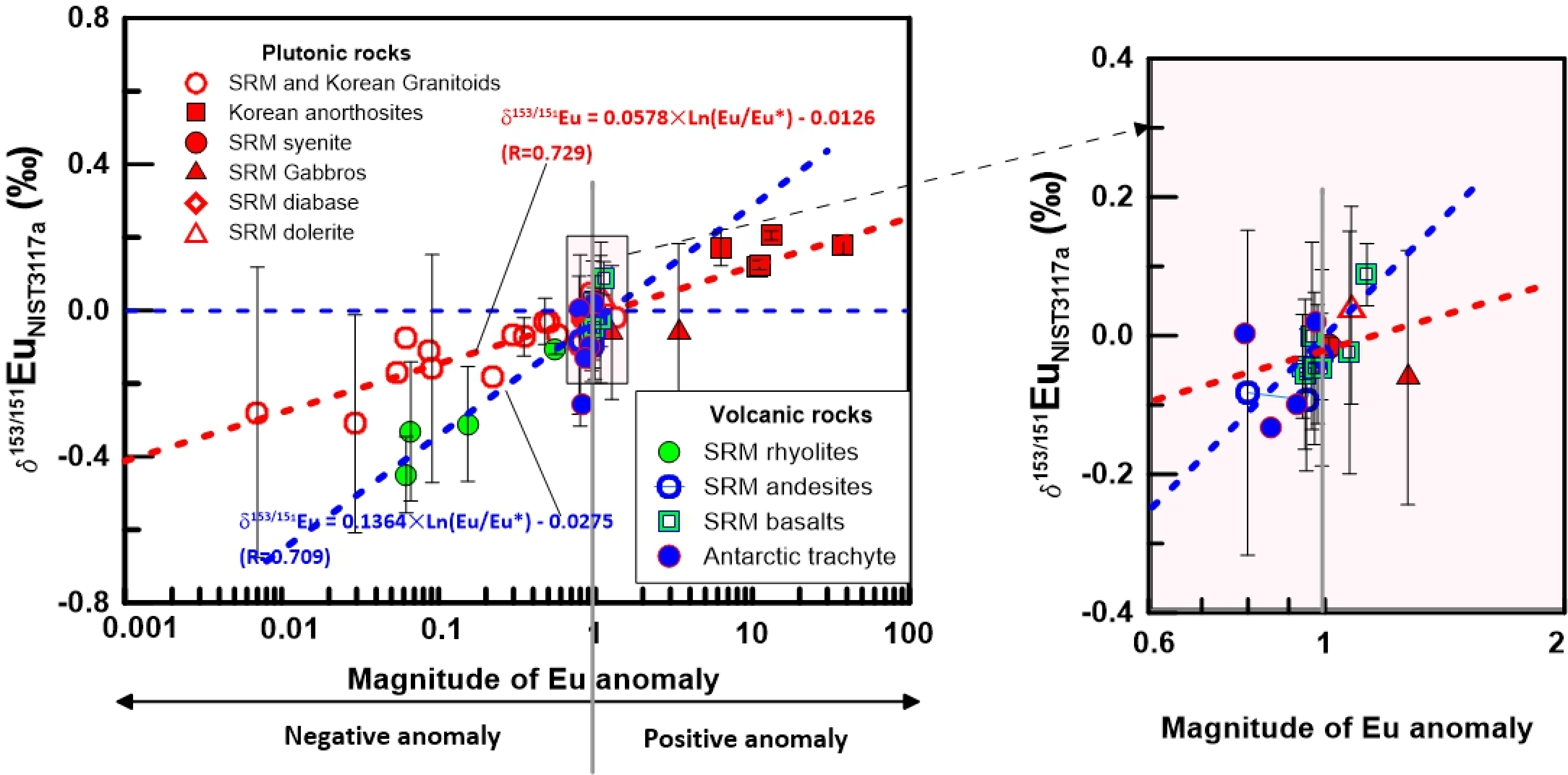

Plutonic rocks
SRM and Korean Granitoids
Korean anorthosites
SRM syenite
SRM Gabbros
SRM diabase
SRM dolerite
$\delta^{153/151}$Eu = 0.0578×Ln(Eu/Eu*) - 0.0126
(R=0.729)
$\delta^{153/151}$Eu = 0.1364×Ln(Eu/Eu*) - 0.0275
(R=0.709)
Volcanic rocks
SRM rhyolites
SRM andesites
SRM basalts
Antarctic trachyte
$\delta^{153/151}Eu_{NIST3117a}$ (‰)
0.8
0.4
0.0
-0.4
-0.8
0.001
0.01
0.1
1
10
100
Magnitude of Eu anomaly
Negative anomaly
Positive anomaly
0.2
-0.2
0.6
2

Table S1. Concentrations of Rare earth element of standard reference materials (SRMs) measured in this study

Type	Sample	La	Ce	Pr	Nd	Sm	Eu	Gd	Tb	Dy	Ho	Er	Tm	Yb	Lu	Eu/Eu*[1]	Ref
basalt	**BCR2[2]**	**25.0**	**53.0**	**6.80**	**28.0**	**6.70**	**2.00**	**6.80**	**1.07**	**6.41**	**1.33**	**3.66**	**0.54**	**3.50**	**0.51**	**0.90**	**USGS**
		25.0 ± 0.9 (n=4, 1σ_m)	53.7 ± 1.1 (n=4, 1σ_m)	6.73 ± 0.16 (n=4, 1σ_m)	28.5 ± 0.6 (n=4, 1σ_m)	6.58 ± 0.15 (n=4, 1σ_m)	2.05 ± 0.04 (n=4, 1σ_m)	6.76 ± 0.17 (n=4, 1σ_m)	1.03 ± 0.03 (n=4, 1σ_m)	6.48 ± 0.13 (n=4, 1σ_m)	1.32 ± 0.03 (n=4, 1σ_m)	3.77 ± 0.09 (n=4, 1σ_m)	0.52 ± 0.01 (n=4, 1σ_m)	3.41 ± 0.05 (n=4, 1σ_m)	0.51 ± 0.01 (n=4, 1σ_m)	0.94	this study
	BHVO2	**15.00**	**38.00**	**-**	**25.00**	**6.20**	**2.05**	**6.30**	**0.90**	**-**	**1.04**	**-**	**-**	**2.00**	**0.28**	**1.00**	**USGS**
		14.9 ± 0.44 (n=3, 1σ_m)	36.2 ± 1.80 (n=3, 1σ_m)	5.17 ± 0.18 (n=3, 1σ_m)	23.2 ± 1.22 (n=3, 1σ_m)	5.76 ± 0.16 (n=3, 1σ_m)	2.05 ± 0.10 (n=3, 1σ_m)	5.90 ± 0.34 (n=3, 1σ_m)	0.97 ± 0.07 (n=3, 1σ_m)	4.89 ± 0.36 (n=3, 1σ_m)	0.97 ± 0.03 (n=3, 1σ_m)	2.39 ± 0.17 (n=3, 1σ_m)	0.26 ± 0.02 (n=3, 1σ_m)	1.66 ± 0.12 (n=3, 1σ_m)	0.25 ± 0.02 (n=3, 1σ_m)	1.07	this study
	BIR1a	**0.63**	**1.90**	**-**	**2.50**	**1.10**	**0.55**	**1.80**	**-**	**4.00**	**-**	**-**	**-**	**1.70**	**0.26**	**1.13**	**USGS**
		0.64 ± 0.05 (n=3, 1σ_m)	1.99 ± 0.10 (n=3, 1σ_m)	0.40 ± 0.05 (n=3, 1σ_m)	2.49 ± 0.08 (n=3, 1σ_m)	1.12 ± 0.05 (n=3, 1σ_m)	0.53 ± 0.02 (n=3, 1σ_m)	1.80 ± 0.23 (n=3, 1σ_m)	0.36 ± 0.03 (n=3, 1σ_m)	2.61 ± 0.20 (n=3, 1σ_m)	0.57 ± 0.05 (n=3, 1σ_m)	1.72 ± 0.17 (n=3, 1σ_m)	0.34 ± 0.03 (n=3, 1σ_m)	1.94 ± 0.05 (n=3, 1σ_m)	0.26 ± 0.01 (n=3, 1σ_m)	1.13	this study
	JB1a	**37.60**	**65.90**	**7.30**	**26.00**	**5.07**	**1.46**	**4.67**	**0.69**	**3.99**	**0.71**	**2.18**	**0.33**	**2.10**	**0.33**	**0.91**	**GSJ**
		33.7 ± 0.8 (n=6, 1σ_m)	74.6 ± 9.7 (n=6, 1σ_m)	6.47 ± 0.18 (n=6, 1σ_m)	24.7 ± 0.6 (n=6, 1σ_m)	4.72 ± 0.11 (n=6, 1σ_m)	1.49 ± 0.03 (n=6, 1σ_m)	4.43 ± 0.10 (n=6, 1σ_m)	0.66 ± 0.01 (n=6, 1σ_m)	3.76 ± 0.16 (n=6, 1σ_m)	0.70 ± 0.02 (n=6, 1σ_m)	2.12 ± 0.05 (n=6, 1σ_m)	0.29 ± 0.01 (n=6, 1σ_m)	1.91 ± 0.05 (n=6, 1σ_m)	0.28 ± 0.01 (n=6, 1σ_m)	0.99	this study
	JB1b	**41.20**	**71.80**	**7.73**	**27.10**	**5.17**	**1.59**	**4.38**	**0.69**	**3.73**	**0.67**	**1.97**	**0.31**	**2.10**	**0.31**	**1.02**	**GSJ**
		40.20	70.10	7.46	26.90	4.93	1.59	5.35	0.77	4.14	0.79	2.22	0.33	2.01	0.31	0.94	this study
	JB2	**2.35**	**6.76**	**1.01**	**6.63**	**2.31**	**0.86**	**3.28**	**0.60**	**3.73**	**0.75**	**2.60**	**0.41**	**2.62**	**0.40**	**0.95**	**GSJ**
		2.18 ± 0.8 (n=8, 1σ_m)	6.39 ± 0.14 (n=8, 1σ_m)	1.11 ± 0.05 (n=8, 1σ_m)	6.26 ± 0.17 (n=8, 1σ_m)	2.22 ± 0.04 (n=8, 1σ_m)	0.83 ± 0.03 (n=8, 1σ_m)	3.09 ± 0.07 (n=8, 1σ_m)	0.56 ± 0.01 (n=8, 1σ_m)	3.77 ± 0.09 (n=8, 1σ_m)	0.81 ± 0.04 (n=8, 1σ_m)	2.51 ± 0.07 (n=8, 1σ_m)	0.37 ± 0.01 (n=8, 1σ_m)	2.42 ± 0.06 (n=8, 1σ_m)	0.37 ± 0.01 (n=8, 1σ_m)	0.96	this study
	JB3	**8.81**	**21.50**	**3.11**	**15.60**	**4.27**	**1.32**	**4.67**	**0.73**	**4.54**	**0.80**	**2.49**	**0.42**	**2.55**	**0.39**	**0.90**	**GSJ**
		8.82 ± 0.70 (n=3, 1σ_m)	22.0 ± 2.5 (n=3, 1σ_m)	3.45 ± 0.35 (n=3, 1σ_m)	16.0 ± 1.78 (n=3, 1σ_m)	4.31 ± 0.35 (n=3, 1σ_m)	1.41 ± 0.16 (n=3, 1σ_m)	4.55 ± 0.56 (n=3, 1σ_m)	0.78 ± 0.07 (n=3, 1σ_m)	4.64 ± 0.73 (n=3, 1σ_m)	1.01 ± 0.12 (n=3, 1σ_m)	2.71 ± 0.44 (n=3, 1σ_m)	0.42 ± 0.05 (n=3, 1σ_m)	2.57 ± 0.22 (n=3, 1σ_m)	0.39 ± 0.05 (n=3, 1σ_m)	0.97	this study
Rhyolite	**JR1**	**19.70**	**47.20**	**5.58**	**23.30**	**6.03**	**0.30**	**5.06**	**1.01**	**5.69**	**1.11**	**3.61**	**0.67**	**4.55**	**0.71**	**0.17**	**GSJ**
		17.35	43.83	5.58	22.52	5.37	0.27	5.48	0.94	6.09	1.25	4.25	0.70	4.94	0.76	0.15	this study
	JR2	**16.30**	**38.80**	**4.75**	**20.40**	**5.63**	**0.14**	**5.83**	**1.10**	**6.63**	**1.39**	**4.36**	**0.74**	**5.33**	**0.88**	**0.07**	**GSJ**
		13.72	37.58	4.53	17.77	4.95	0.09	5.29	0.98	6.39	1.41	4.42	0.74	5.08	0.81	0.05	this study
	JR3	**179**	**327**	**33.1**	**107**	**21.3**	**0.53**	**19.7**	**4.29**	**21.5**	**4.70**	**14.0**		**20.3**	**2.80**	**0.06**	**GSJ**
		167 ± 5 (n=4, 1σ_m)	309 ± 9 (n=4, 1σ_m)	30.9 ± 1.5 (n=4, 1σ_m)	101 ± 3 (n=4, 1σ_m)	20.1 ± 0.7 (n=4, 1σ_m)	0.41 ± 0.02 (n=4, 1σ_m)	20.2 ± 0.72 (n=4, 1σ_m)	3.99 ± 0.25 (n=4, 1σ_m)	27.1 ± 1.3 (n=4, 1σ_m)	6.00 ± 0.33 (n=4, 1σ_m)	18.3 ± 0.7 (n=4, 1σ_m)	2.96 ± 0.18 (n=4, 1σ_m)	19.0 ± 0.8 (n=4, 1σ_m)	2.71 ± 0.07 (n=4, 1σ_m)	0.06	this study
	RGM2	**25.00**	**48.00**	**5.00**	**20.00**	**4.00**	**0.70**	**3.60**	**0.60**	**3.30**	**0.80**	**2.20**			**0.40**	**0.56**	**USGS**
		22.7 ± 1.8 (n=2, 1σ_m)	47.2 ± 1.0 (n=2, 1σ_m)	5.27 ± 0.31 (n=2, 1σ_m)	19.4 ± 0.90 (n=2, 1σ_m)	3.91 ± 0.48 (n=2, 1σ_m)	0.70 ± 0.03 (n=2, 1σ_m)	3.81 ± 0.31 (n=2, 1σ_m)	0.57 ± 0.02 (n=2, 1σ_m)	3.60 ± 0.19 (n=2, 1σ_m)	0.73 ± 0.06 (n=2, 1σ_m)	2.33 ± 0.09 (n=2, 1σ_m)	0.36 ± 0.00 (n=2, 1σ_m)	0.52 ± 0.09 (n=2, 1σ_m)	0.38 ± 0.01 (n=2, 1σ_m)	0.56	this study
Andesite	**JA1**	**5.24**	**13.30**	**1.71**	**10.90**	**3.52**	**1.20**	**4.36**	**0.75**	**4.55**	**0.95**	**3.04**	**0.47**	**3.03**	**0.47**	**0.93**	**GSJ**
		4.69 ± 0.06 (n=6, 1σ_m)	11.8 ± 1.52 (n=6, 1σ_m)	2.01 ± 0.04 (n=6, 1σ_m)	10.7 ± 0.2 (n=6, 1σ_m)	3.30 ± 0.03 (n=6, 1σ_m)	1.16 ± 0.02 (n=6, 1σ_m)	4.31 ± 0.05 (n=6, 1σ_m)	0.72 ± 0.01 (n=6, 1σ_m)	4.65 ± 0.12 (n=6, 1σ_m)	0.94 ± 0.01 (n=6, 1σ_m)	3.04 ± 0.02 (n=6, 1σ_m)	0.44 ± 0.00 (n=6, 1σ_m)	2.91 ± 0.02 (n=6, 1σ_m)	0.44 ± 0.00 (n=6, 1σ_m)	0.93	this study
	JA2	**15.80**	**32.70**	**3.84**	**13.90**	**3.11**	**0.93**	**3.06**	**0.44**	**2.80**	**0.50**	**1.48**	**0.28**	**1.62**	**0.27**	**0.92**	**GSJ**
		14.5 ± 0.25 (n=6, 1σ_m)	28.8 ± 3.9 (n=6, 1σ_m)	3.48 ± 0.05 (n=6, 1σ_m)	13.8 ± 0.2 (n=6, 1σ_m)	2.93 ± 0.04 (n=6, 1σ_m)	0.92 ± 0.02 (n=6, 1σ_m)	2.99 ± 0.03 (n=6, 1σ_m)	0.46 ± 0.00 (n=6, 1σ_m)	2.78 ± 0.04 (n=6, 1σ_m)	0.54 ± 0.01 (n=6, 1σ_m)	1.69 ± 0.04 (n=6, 1σ_m)	0.25 ± 0.00 (n=6, 1σ_m)	1.59 ± 0.03 (n=6, 1σ_m)	0.24 ± 0.01 (n=6, 1σ_m)	0.95	this study
	JA3	**9.33**	**22.80**	**2.40**	**12.30**	**3.05**	**0.82**	**2.96**	**0.52**	**3.01**	**0.51**	**1.57**	**0.28**	**2.16**	**0.27**	**0.83**	**GSJ**
		8.91 ± 0.25 (n=6, 1σ_m)	21.0 ± 3.9 (n=6, 1σ_m)	2.74 ± 0.05 (n=6, 1σ_m)	12.2 ± 0.2 (n=6, 1σ_m)	3.02 ± 0.04 (n=6, 1σ_m)	0.82 ± 0.02 (n=6, 1σ_m)	3.23 ± 0.03 (n=6, 1σ_m)	0.51 ± 0.00 (n=6, 1σ_m)	3.21 ± 0.04 (n=6, 1σ_m)	0.65 ± 0.01 (n=6, 1σ_m)	1.99 ± 0.04 (n=6, 1σ_m)	0.29 ± 0.00 (n=6, 1σ_m)	1.94 ± 0.03 (n=6, 1σ_m)	0.29 ± 0.01 (n=6, 1σ_m)	0.80	this study
	AGV2	**38.00**	**68.00**	**8.30**	**30.00**	**5.70**	**1.54**	**4.69**	**0.64**	**3.60**	**0.71**	**1.79**	**0.26**	**1.60**	**0.25**	**0.91**	**USGS**
		29.3 ± 0.4 (n=6, 1σ_m)	74.6 ± 10.5 (n=6, 1σ_m)	6.26 ± 0.08 (n=6, 1σ_m)	24.2 ± 0.25 (n=6, 1σ_m)	4.39 ± 0.05 (n=6, 1σ_m)	1.41 ± 0.16 (n=6, 1σ_m)	4.55 ± 0.56 (n=6, 1σ_m)	0.78 ± 0.07 (n=6, 1σ_m)	4.64 ± 0.73 (n=6, 1σ_m)	1.01 ± 0.12 (n=6, 1σ_m)	2..71 ± 0.44 (n=6, 1σ_m)	0.42 ± 0.05 (n=6, 1σ_m)	2.57 ± 0.22 (n=6, 1σ_m)	0.39 ± 0.05 (n=6, 1σ_m)	0.96	this study
	G2	**89.0**	**160**	**18.0**	**55.0**	**7.20**	**1.40**	**4.30**	**0.48**	**2.40**	**0.40**	**0.92**	**0.18**	**0.48**	**0.11**	**0.78**	**USGS**
		96.1 ± 12.1 (n=2, 1σ_m)	160 ± 2 (n=2, 1σ_m)	16.1 ± 1.1 (n=2, 1σ_m)	53.0 ± 1.3 (n=2, 1σ_m)	7.18 ± 0.06 (n=2, 1σ_m)	1.55 ± 0.09 (n=2, 1σ_m)	4.07 ± 0.17 (n=2, 1σ_m)	0.47 ± 0.01 (n=2, 1σ_m)	2.13 ± 0.16 (n=2, 1σ_m)	0.32 ± 0.04 (n=2, 1σ_m)	0.89 ± 0.02 (n=2, 1σ_m)	0.10 ± 0.05 (n=2, 1σ_m)	0.66 ± 0.11 (n=2, 1σ_m)	0.07 ± 0.02 (n=2, 1σ_m)	0.86	this study

Granite	**GSP2**	**180**	**410**	**51.0**	**200**	**27.0**	**2.30**	**12.0**	**1.40**	**6.10**	**1.00**	**2.20**	**0.30**	**1.60**	**0.23**	**0.39**	**USGS**
		176 ± 19 (n=4, $1\sigma_m$)	453 ± 30 (n=4, $1\sigma_m$)	53.1 ± 4.4 (n=4, $1\sigma_m$)	197 ± 15 (n=4, $1\sigma_m$)	25.6 ± 1.5 (n=4, $1\sigma_m$)	2.30 ± 0.11 (n=4, $1\sigma_m$)	12.1 ± 0.6 (n=4, $1\sigma_m$)	1.29 ± 0.06 (n=4, $1\sigma_m$)	5.82 ± 0.27 (n=4, $1\sigma_m$)	0.94 ± 0.03 (n=4, $1\sigma_m$)	2.34 ± 0.09 (n=4, $1\sigma_m$)	0.27 ± 0.01 (n=4, $1\sigma_m$)	1.61 ± 0.03 (n=4, $1\sigma_m$)	0.22 ± 0.01 (n=4, $1\sigma_m$)	0.40	this study
	JG1a	**21.30**	**45.00**	**5.63**	**20.40**	**4.53**	**0.70**	**4.10**	**0.81**	**4.44**	**0.82**	**2.57**	**0.38**	**2.70**	**0.44**	**0.50**	**GSJ**
		20.9 ± 0.69 (n=5, $1\sigma_m$)	45.0 ± 1.9 (n=5, $1\sigma_m$)	5.02 ± 0.11 (n=5, $1\sigma_m$)	19.2 ± 0.5 (n=5, $1\sigma_m$)	4.32 ± 0.11 (n=5, $1\sigma_m$)	0.68 ± 0.02 (n=5, $1\sigma_m$)	4.21 ± 0.16 (n=5, $1\sigma_m$)	0.72 ± 0.03 (n=5, $1\sigma_m$)	4.70 ± 0.24 (n=5, $1\sigma_m$)	0.96 ± 0.06 (n=5, $1\sigma_m$)	2.90 ± 0.17 (n=5, $1\sigma_m$)	0.44 ± 0.03 (n=5, $1\sigma_m$)	2.98 ± 0.22 (n=5, $1\sigma_m$)	0.43 ± 0.03 (n=5, $1\sigma_m$)	0.48	this study
	JG2	**19.90**	**48.30**	**6.20**	**26.40**	**7.78**	**0.10**	**8.01**	**1.62**	**10.50**	**1.67**	**6.04**	**1.16**	**6.85**	**1.22**	**0.04**	**GSJ**
		19.0 ± 0.72 (n=4, $1\sigma_m$)	49.6 ± 1.3 (n=4, $1\sigma_m$)	6.00 ± 0.26 (n=4, $1\sigma_m$)	24.4 ± 0.75 (n=4, $1\sigma_m$)	7.97 ± 0.22 (n=4, $1\sigma_m$)	0.08 ± 0.02 (n=4, $1\sigma_m$)	9.63 ± 0.47 (n=4, $1\sigma_m$)	1.87 ± 0.13 (n=4, $1\sigma_m$)	12.4 ± 0.8 (n=4, $1\sigma_m$)	2.69 ± 0.17 (n=4, $1\sigma_m$)	8.01 ± 0.38 (n=4, $1\sigma_m$)	1.26 ± 0.07 (n=4, $1\sigma_m$)	8.11 ± 0.39 (n=4, $1\sigma_m$)	1.21 ± 0.07 (n=4, $1\sigma_m$)	0.03	this study
	JG3	**20.60**	**40.30**	**4.70**	**17.20**	**3.39**	**0.90**	**2.92**	**0.46**	**2.59**	**0.38**	**1.52**	**0.24**	**1.77**	**0.26**	**0.87**	**GSJ**
		19.7 ± 0.23 (n=6, $1\sigma_m$)	37.2 ± 4.8 (n=6, $1\sigma_m$)	4.47 ± 0.07 (n=6, $1\sigma_m$)	16.9 ± 0.03 (n=6, $1\sigma_m$)	3.20 ± 0.03 (n=6, $1\sigma_m$)	0.91 ± 0.02 (n=6, $1\sigma_m$)	2.95 ± 0.02 (n=6, $1\sigma_m$)	0.44 ± 0.01 (n=6, $1\sigma_m$)	2.64 ± 0.03 (n=6, $1\sigma_m$)	0.50 ± 0.00 (n=6, $1\sigma_m$)	1.58 ± 0.01 (n=6, $1\sigma_m$)	0.23 ± 0.00 (n=6, $1\sigma_m$)	1.60 ± 0.02 (n=6, $1\sigma_m$)	0.24 ± 0.00 (n=6, $1\sigma_m$)	0.90	this study
diabase	**W2a**	**10.00**	**23.00**	**-**	**13.00**	**3.30**	**1.00**	**-**	**0.63**	**3.60**	**0.76**	**2.50**	**0.38**	**2.10**	**0.33**	**-**	**USGS**
		10.0 ± 0.07 (n=6, $1\sigma_m$)	20.6 ± 2.8 (n=6, $1\sigma_m$)	2.86 ± 0.02 (n=6, $1\sigma_m$)	12.7 ± 0.06 (n=6, $1\sigma_m$)	3.19 ± 0.04 (n=6, $1\sigma_m$)	1.12 ± 0.02 (n=6, $1\sigma_m$)	3.76 ± 0.05 (n=6, $1\sigma_m$)	0.60 ± 0.01 (n=6, $1\sigma_m$)	3.74 ± 0.04 (n=6, $1\sigma_m$)	0.72 ± 0.01 (n=6, $1\sigma_m$)	2.23 ± 0.01 (n=6, $1\sigma_m$)	0.32 ± 0.00 (n=6, $1\sigma_m$)	2.02 ± 0.02 (n=6, $1\sigma_m$)	0.30 ± 0.01 (n=6, $1\sigma_m$)	0.98	this study
dolerite	**DNC1a**	**3.60**		**1.20**	**5.20**	**1.41**	**0.59**	**2.00**	**0.42**	**3.00**	**0.62**	**1.70**	**0.33**	**2.00**	**0.27**	**1.07**	**USGS**
		4.20 ± 0.39 (n=4, $1\sigma_m$)	10.3 ± 0.9 (n=4, $1\sigma_m$)	1.37 ± 0.12 (n=4, $1\sigma_m$)	6.31 ± 0.57 (n=4, $1\sigma_m$)	1.80 ± 0.17 (n=4, $1\sigma_m$)	0.77 ± 0.08 (n=4, $1\sigma_m$)	2.61 ± 0.25 (n=4, $1\sigma_m$)	0.48 ± 0.04 (n=4, $1\sigma_m$)	3.40 ± 0.25 (n=4, $1\sigma_m$)	0.74 ± 0.03 (n=4, $1\sigma_m$)	2.47 ± 0.22 (n=4, $1\sigma_m$)	0.37 ± 0.03 (n=4, $1\sigma_m$)	2.44 ± 0.20 (n=4, $1\sigma_m$)	0.38 ± 0.03 (n=4, $1\sigma_m$)	1.08	this study
syenite	**STM2**	**154**	**256**	**25.0**	**81.0**	**12.0**	**3.45**	**8.00**	**1.38**	**8.01**	**1.55**	**4.40**	**0.55**	**4.20**	**0.60**	**1.07**	**USGS**
		153 ± 5 (n=2, $1\sigma_m$)	258 ± 17 (n=2, $1\sigma_m$)	26.8 ± 0.9 (n=2, $1\sigma_m$)	79.5 ± 7 (n=2, $1\sigma_m$)	12.5 ± 0.3 (n=2, $1\sigma_m$)	3.72 ± 0.08 (n=2, $1\sigma_m$)	12.5 ± 0.1 (n=2, $1\sigma_m$)	1.30 ± 0.28 (n=2, $1\sigma_m$)	7.90 ± 0.11 (n=2, $1\sigma_m$)	1.54 ± 0.07 (n=2, $1\sigma_m$)	4.25 ± 0.05 (n=2, $1\sigma_m$)	0.66 ± 0.04 (n=2, $1\sigma_m$)	0.69 ± 0.13 (n=2, $1\sigma_m$)	0.06 ± 0.00 (n=2, $1\sigma_m$)	1.01	this study
gabbro	**JGb1**	**3.60**	**8.17**	**1.13**	**5.47**	**1.49**	**0.62**	**1.61**	**0.29**	**1.56**	**0.33**	**1.04**	**0.16**	**1.06**	**0.15**	**1.22**	**GSJ**
		3.40 ± 0.09 (n=5, $1\sigma_m$)	7.55 ± 1.2 (n=5, $1\sigma_m$)	1.12 ± 0.03 (n=5, $1\sigma_m$)	5.29 ± 0.14 (n=5, $1\sigma_m$)	1.40 ± 0.04 (n=5, $1\sigma_m$)	0.61 ± 0.01 (n=5, $1\sigma_m$)	1.52 ± 0.19 (n=5, $1\sigma_m$)	0.27 ± 0.01 (n=5, $1\sigma_m$)	1.70 ± 0.12 (n=5, $1\sigma_m$)	0.33 ± 0.03 (n=5, $1\sigma_m$)	1.00 ± 0.07 (n=5, $1\sigma_m$)	0.14 ± 0.01 (n=5, $1\sigma_m$)	0.92 ± 0.04 (n=5, $1\sigma_m$)	0.13 ± 0.01 (n=5, $1\sigma_m$)	1.27	this study
	JGb2	**1.50**	**3.00**	**0.39**	**1.80**	**0.51**	**0.59**	**0.48**	**0.15**	**0.60**	**0.15**	**0.36**	**0.06**	**0.39**	**0.06**	**3.63**	**GSJ**
		1.28 ± 0.13 (n=2, $1\sigma_m$)	2.27 ± 0.42 (n=2, $1\sigma_m$)	0.37 ± 0.01 (n=2, $1\sigma_m$)	1.74 ± 0.04 (n=2, $1\sigma_m$)	0.49 ± 0.01 (n=2, $1\sigma_m$)	0.59 ± 0.00 (n=2, $1\sigma_m$)	0.58 ± 0.06 (n=2, $1\sigma_m$)	0.10 ± 0.03 (n=2, $1\sigma_m$)	0.63 ± 0.02 (n=2, $1\sigma_m$)	0.12 ± 0.01 (n=2, $1\sigma_m$)	0.40 ± 0.02 (n=2, $1\sigma_m$)	0.06 ± 0.00 (n=2, $1\sigma_m$)	0.39 ± 0.00 (n=2, $1\sigma_m$)	0.06 ± 0.00 (n=2, $1\sigma_m$)	3.38	this study

[1)] The magnitude of Eu anomaly is defined as s the ratio Eu_N/Eu^* where Eu^* is SQRT(Sm_N x Gd_N). The magnitude was calculated based on the values of Sm, Eu and Gd from the reference.

[2)] The bold number of this raw are recommended value by United States of Geological Survey (USGS) or Geological Survey of Japan (GSJ)